

Original

Riekehr, S.; Ravasi, R.; Enz, J.; Ventzke, V.; Kashaev, N.:

Mechanical Properties of Fibre Laser Welded AZ31B Sheets and their Dependence on the Spot-Size

Materials Science Forum, Light Metals Technology 2015 (2015)

Trans Tech Publications

DOI: [10.4028/www.scientific.net/MSF.828-829.298](https://doi.org/10.4028/www.scientific.net/MSF.828-829.298)

Mechanical Properties of Fibre Laser Welded AZ31B Sheets and their Dependence on the Spot-size

STEFAN Riekehr^{a*}, RICARDO Ravasi^b, JOSEPHIN Enz^c, VOLKER VENTZKE^d
and NIKOLAI KASHAEV^e

Helmholtz-Zentrum Geesthacht, Institute of Materials Research, Materials Mechanics / ACE
Centre, Max-Planck-Strasse 1, D-21502 Geesthacht, Germany

^astefan.riekehr@hzg.de, ^bricardo.ravasi@hzg.de, ^cjosephin.enz@hzg.de, ^dvolker.ventzke@hzg.de,
^enikolai.kashaev@hzg.de

Keywords: laser beam welding, magnesium, AZ31, weldability, remote welding, mechanical parameter.

Abstract: In the present work the mechanical behaviour of laser beam welded AZ31B alloy was studied, by changing systematically the spot size of the used fibre laser system between 200 µm and 1000 µm at different power levels between 2 kW and 8 kW. Maximum welding velocities with respect to imperfections were determined. The characterization of the obtained welds - in terms of Vickers hardness, UTS, A_f and weld width, resp. weld area - was correlated with the micro-texture in dependence of the different Focus Spot Diameters and Laser Beam Power levels as well as the resulting cooling rates. Highest UTS of 94% of the base material was achieved with 200 µm Focus Spot Diameter and Laser Beam Power of 4 kW at welding velocity of 100 mm/s. By increasing the Focus Spot Diameter to 600 µm, the tensile strength was reduced to 86 % of the actual strength of the base material.

Introduction

The joining of magnesium alloys is well understood and good welds with strength levels close to that of the base material (BM) are achieved easily. However, the deformation capacity of the welded joints - especially of the primarily used AZ31 - is well below the BM level [1-3].

By new developments such as remote welding, the spot size of the laser comes back into the focus of scientific interest. New brilliant laser sources can deliver several kW via fibres with diameters of a few tenths of millimetres. In the close up, very small spots can be realized, but for sheet applications, where butt welding is mainly used and the demands of proper edge preparation are raising, the zero-gap is necessary. In undermatched welds, small weld zones may improve the mechanical behaviour by bridging of BM properties over the weld: However requirements like gap bridging capability of the process may lead to larger welds with inferior strength.

Base material. The AZ31B sheets were produced by POSCO and were delivered as sheets with dimensions of 1300x400x2 mm. The chemical composition of the AZ31B sheets was measured with a DIA200SE and is listed in Table 1. For the determination of tensile properties the average value of three tested specimens was calculated. Tests were performed in an electro-mechanical universal testing machine (Schenck RM100) according to ISO 6892-1:2009. Results are tabulated in Table 2.

Table 1. Chemical composition of magnesium alloy AZ31B.

Element	Al	Zn	Mn	Si	Cu	Ni	Fe	Ca	Other	Mg
wt.%	3.07	0.774	0.358	0.051	0.0008	0.0014	0.0024	0.0006	<0.3	balance

Table 2. Tensile properties of magnesium alloy AZ31B (acc. DIN EN ISO 6892-1:2009)

Specimen orientation	R _{p0.2} [MPa]	R _m [MPa]	A _f [%]
Transversal direction	206.8	274.2	10.6
Longitudinal direction	222.5	276.0	9.0

Fibre laser beam welding

Equipment. An 8 kW fibre laser (IPG YLS-8000) was used for butt welding of the AZ31B sheets. In order to achieve different spot diameters, three different fibres with core diameters of 100 μm , 200 μm and 300 μm were used. All fibres were attached to a Precitec YW52 laser head mounted on an industrial 6-axis KUKA robot arm, with a payload of 30 kg (KUKA KR30HA). The characteristic data of the used laser system are summarized in Table 3.

Table 3. Laser system characteristics

	Maximum Power [kW]	Wavelength [nm]	Beam Parameter Product [mm*mrad]	Fibre diameter [μm]	Focal length [mm]	Collimator length [mm]	Laser spot [μm]
Ytterbium Laser System YLS-8000	8	1060-1080	3.7	100	300	150	200
			7.5	200	300	150	400
			11.4	300	300	150	600
				300	500	150	1000

The welding velocities used were in the range between 0.05 and 0.2 m/s, which are relatively low paces. The maximum linear velocity of the robot system is 2 m/s. The pose accuracy of the used system is ± 0.05 mm, which is highly accurate for an industrial robot. In combination with decreasing Focus Spot Diameters (FSD) the importance of high pose accuracy will possibly grow in the future.

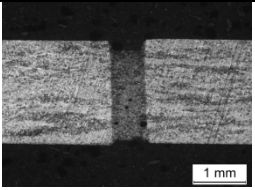
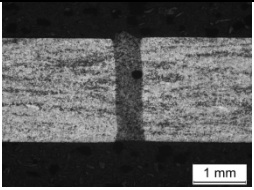
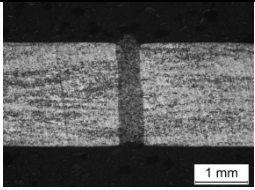
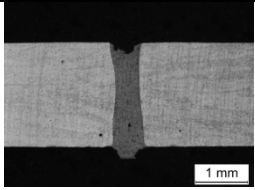
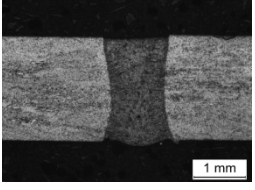
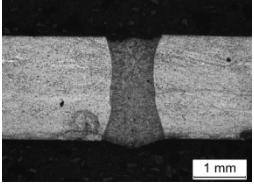
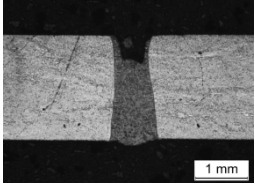
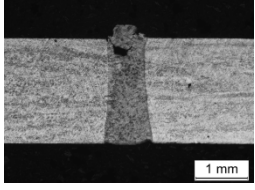
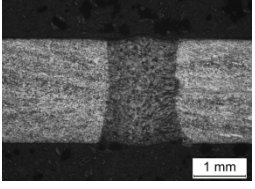
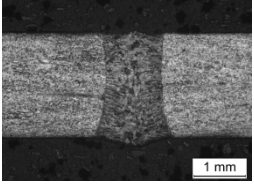
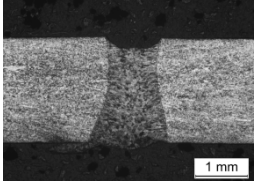
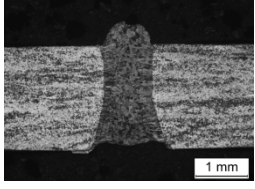
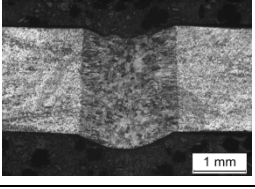
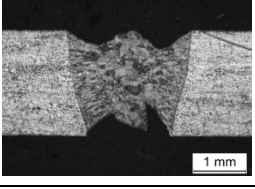
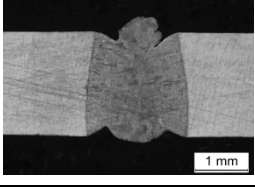
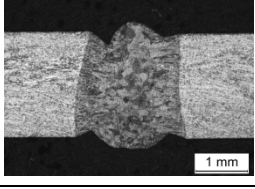
Welding. Laser beam welding was performed at FSD of 200 μm , 400 μm , 600 μm and 1000 μm and Laser Beam Powers (LBP) of 2 kW, 4 kW, 6 kW and 8 kW were used. The best set of parameters found was used for an analysis of gap-bridging capacity by opening a gap of up to 0.4 mm. In Table 4 the parameter matrix is shown with related cross sections. For different LBP levels an adequate velocity was chosen to weld all specimens with constant energy input per unit length of 40 J/mm. Preliminary trials showed, that 40 J/mm lead to the best welding results in terms of porosity and spatter. In [1] the best welding parameters were found at energy input per unit length of 44 J/mm. This confirms the study of Wang et al. [4] who recommended energy input per unit length below 48 J/mm for fibre laser beam welding AZ31. Despite of the constant energy input per unit length, the weld bead width is growing with increasing spot diameter and it is decreasing with increasing velocity, as can be seen in Table 4. Comparing welds just by the energy input per unit length, as it is common for conventional welds, is not possible for laser beam welding, when the focus diameter can be widely changed. The change from 200 μm to 1000 μm FSD will lead to a 25 times larger area, where the laser radiation interacts with the material. Nevertheless, the energy density is high enough to stay in the keyhole welding mode, but larger area is pre-heated by the larger FSD, so a larger melt pool with more homogenous temperature distribution will be received. All specimens were welded normal to the rolling direction. Argon was used as shielding gas for the surface and Helium for the root of the weld. The focal plane was placed on the sheet surface.

Characterization of the welds

All welds were assessed according to EN ISO 17636-1 and EN 13919 by visual inspection and X-ray methods. Porosity level and existence of undercuts were the main parameters and the existing porosity was rated to level B, which is the most restrictive level in the EN13919. It must be

mentioned that LBP of 8 kW at all FSDs did not lead to stable welds. Also welding with a FSD of 1000 μm with power levels higher than 2 kW led to instabilities, which were mainly expressed as undercuts and blow outs. A possible explanation could be that with raising laser beam power the temperature gradient in the weld pool is growing and due to this augmented and faster movement in the melt pool will occur, driven by decreasing viscosity [5] and convection. The increase of the welding velocity will lead to higher cooling rates, respectively to faster solidification. It is obvious then, that the combination of higher power and higher velocity will lead to more instabilities in the process.

Table 4. Cross sections of AZ31B laser beam welds with energy input per unit length of 40 J/mm

Focus Spot Diameter	Power - Velocity 2 kW – 50 mm/s	4 kW – 100 mm/s	6 kW – 150 mm/s	8 kW – 200 mm/s
200 μm				
400 μm				
600 μm				
1000 μm				

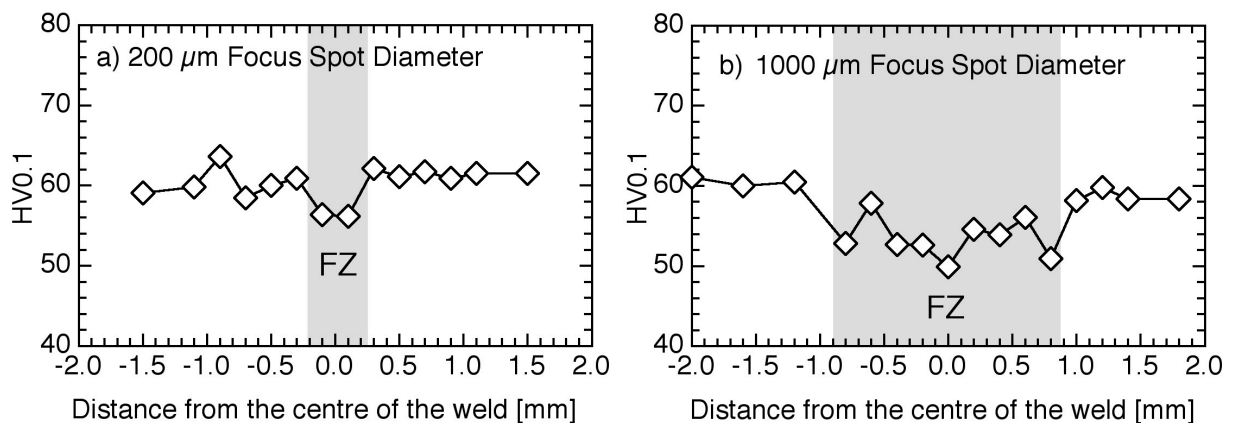


Fig. 1. Microhardness of 2 kW welds with a) 200 μm and b) 1000 μm FSD

Microhardness. The microhardness HV0.1 was determined with a HMV-2000 Hardness Tester from Struers, according to ISO 6507-1:2004. A line of hardness indentations was performed 0.85 mm below the surface. Spacing between the indentations was 200 μm . The BM shows a microhardness of approximately 60HV0.1. The fusion zone (FZ) shows softening and thus the width of the FZ can easily be determined. In Fig. 1 microhardness is plotted for 2 kW LBP with 200 μm and 1000 μm FSD. The weld performed at LBP 2 kW with the FSD 200 μm exhibits a drop of hardness of 10 %, to 56HV0.1, whereas the weld performed at LBP 2 kW with FSD 1000 μm weld reaches only 51HV0.1, equalling 80 % of the BM value, with two distinct minima at the fusion line. Since the same energy input per unit length was used, EBSD micro texture analysis was performed to evaluate differences in grain size and micro texture.

Micro-texture by EBSD. Electron-back-scatter-diffraction (EBSD) was performed in a JEOL JSM-6490LV scanning electron microscope. The specimens were ground and polished manually, necessary etching was done with a mixture of picric and acetic acid for less than 5 seconds.

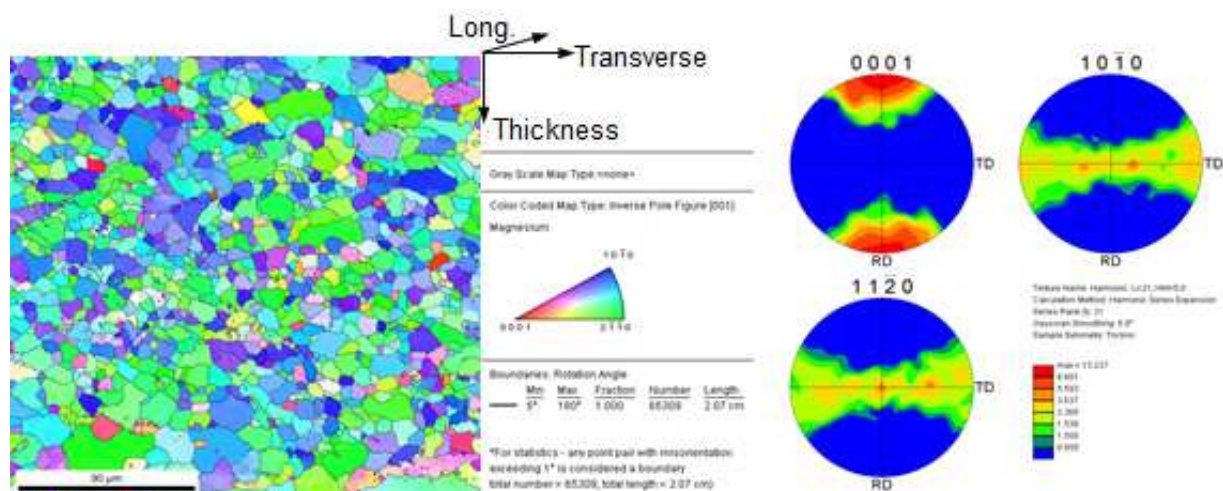


Fig. 2. Base material micro texture: Orientation map and pole figures ($P_{\max} = 13.2$ mrd)

The view of Fig. 2 is in rolling direction, the transverse direction being the width of the picture. The BM exhibits the typical strong basal texture of rolled AZ31B, C-axis is tilting about 20° and the average grain size was 12 μm . The pole figures shows the presence of a $\langle 0\ 0\ 0\ 1 \rangle // \text{RD}$ rotation texture and $(0\ 0\ 0\ 1)[1\ -1\ 2\ 0]$ in the examined AZ31B sheet.

For four welds with LBP of 2 kW and increasing FSD from 200 μm to 1000 μm mapping sequences were completed, to receive an overview of the change of grain size and micro texture from the middle of the fusion zone to the BM, see Fig. 3, from the left to the right in Fig. 3 a) to d).

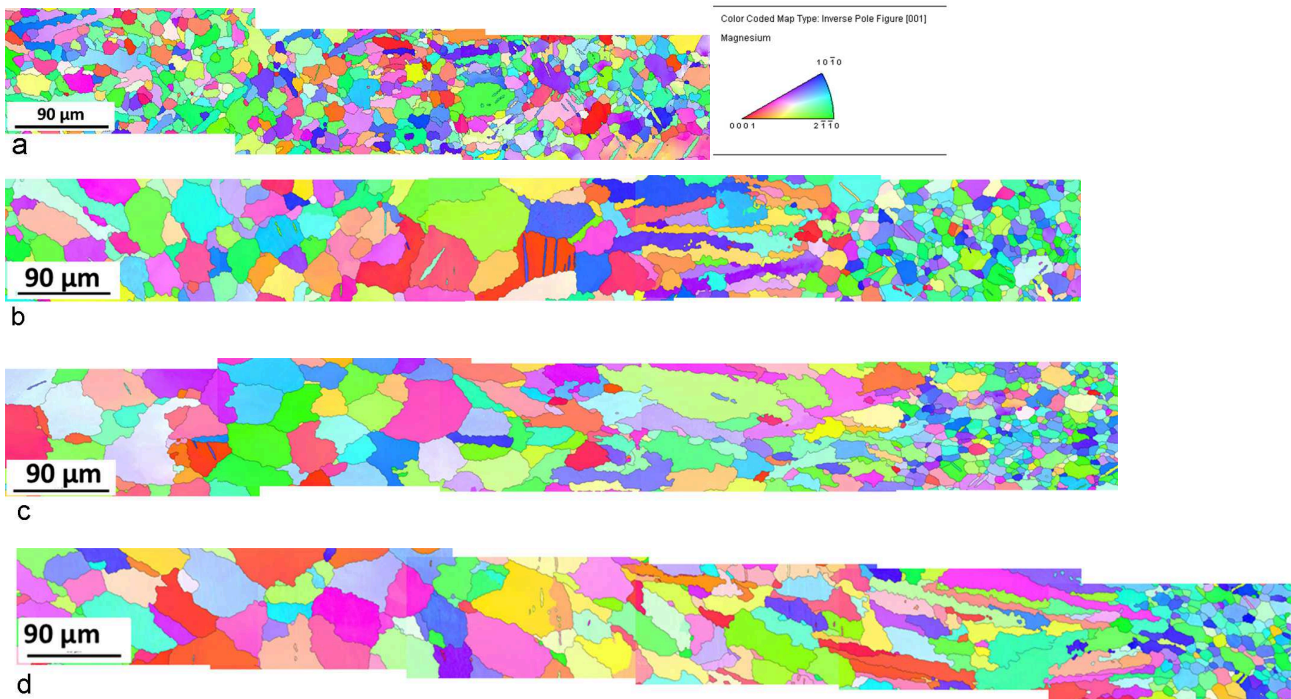


Fig. 3. Orientation maps from middle of the fusion zone to BM. All welds performed at LBP 2 kW and 50 mm/s welding velocity: a) 200 μm FSD, b) 400 μm FSD, c) 600 μm FSD, d) 1000 μm FSD.

With increasing FSD the grain size in the fusion zone is increasing from 17 μm (at 200 μm FSD), and 34 μm to 41 μm and finally to 46 μm (at 1000 μm FSD). So the above mentioned drops in hardness for the weld with 200 μm and 1000 μm can be explained by the grain size and the Hall-Petch mechanism. In finer grains deformation is more often blocked by grain boundaries and, therefore, higher hardness is shown.

In Fig. 3a) the fusion line is hard to determine, Fig. 3b) – d) show an area of long dendritic grains, followed by large equiaxed grains in the centre of the weld zone. This can be explained by different cooling rates for the different welds. The keyhole, typical for laser beam welding, will form close to the centre of the focus spot, with a shifting in welding direction. The keyhole is, more or less, a cylindrical volume of vaporized metal and is kept open by the continuous supplement of energy from the laser beam and the vapour pressure. It is surrounded by molten material.

It is obvious that the temperature gradient within the molten zone will be higher with decreasing width, so less material is molten and less heat energy is stored. Therefore with decreasing FSD the cooling rate will increase and the resulting grain size will be smaller. Overall the cooling rate was high enough that no secondary arms of the dendrites could have grown. As expected, the micro texture changed by welding from the mentioned strong basal texture to a statistically distributed texture. Due to this statistical distribution, more slip systems can be activated in the weld zone and deformation will concentrate in the weld zone, especially in the large equiaxed grains.

Tensile Testing. Tensile tests in the as-welded state were performed in the same way as aforementioned for the BM. All specimens failed in the fusion zone.

The results are shown in Fig. 4. In Fig. 4a the FSD was selected as comparative parameter. It can be stated, that for LBP of 2 kW a spot diameter between 200 μm and 600 μm has no influence on the UTS. The broad weld obtained with 1000 μm spot diameter showed overall lower UTS which additionally decreases with increasing power, from 80 % at 2 kW to 70 % at 8 kW. At 6 kW it is even lower, due to the instable welding conditions of the large spot diameter.

At a power of 4 kW the welds with spot diameters of 200 – 600 μm exhibit a maximum of UTS, with 400 and 600 μm being at the same level of 250 MPa, resp. 90 % of BM and the 200 μm spot even higher with 265 MPa, resp. 96 % of BM. With increasing power the UTS of the 200 μm welds drops slightly to 255 MPa at 8 kW, which is still higher than all results of the larger spot diameters. So a small FSD in combination with a medium power seems advantageous in terms of UTS.

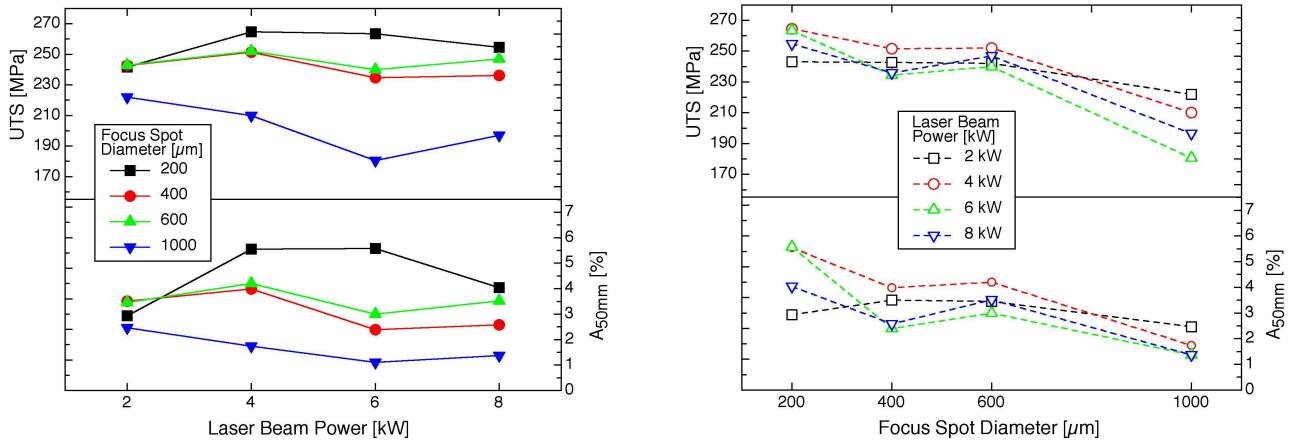


Fig. 4. Tensile strength UTS and percentage elongation to fracture A_{50mm} , $l_0=50$ mm, as function of
 a) Laser Beam Power and
 b) Focus Spot Diameter

In terms of elongation-to-fracture, as displayed in Fig. 4a, a broad weld with undercuts as obtained by 1000 μm FSD led to a low A_f value, which was also dropping with increasing power. This is, as mentioned before, a sign for increasing welding instabilities with increasing power. The use of other FSDs led to an enhancement of A_f when power was increased from 2 kW to 4 kW further power enhancement led to lower A_f values for all FSDs except the 200 μm , which showed stable values for A_f at 4 kW and 6 kW, but dropped at 8 kW.

The behaviour is similar for UTS and A_f . This could be caused by the increasing instability of welding, as mentioned before. Higher laser welding power and higher welding velocity led to smaller welds, as can be seen in Table 3, following the rows from left to right. It must be kept in mind that all specimens were welded with the same energy input per unit length. Higher LBP always means higher welding velocity and from this, it can be concluded that the cooling rates grow, because of the shrinking time interval in which the LBP can affect the material.

Fig. 4b) refers to the LBP as comparative parameter. It can be seen that UTS and A_f present a downward trend with increasing FSD. Only the weld with LBP of 2 kW exhibits a plateau, respectively a maximum at 400 – 600 μm FSD. Due to the smaller weld zone the geometrical imperfections influence on the resulting UTS and A_f could be smaller and micro texture and grain size gain of influence. As mentioned before the statistical distribution of the orientation in the weld zone could offer more deformation capacity.

Generally a larger FSD leads to a broader weld, when LBP is kept constant. With increasing spot diameter the energy density in the spot will decrease and therefore instabilities of the keyhole could occur more easily. On the other hand this effect could be used for gap bridging in industrial applications since 600 μm focus spot size is a value relatively wide used in the remote laser welding applications. The loss of UTS is only 15 %, but the loss of 60 % in global ductility A_f , must be taken into account during the construction.

Conclusions

- Equal energy inputs per unit length during welding lead to differing results. For this reason the energy input per unit length is not a sufficient welding parameter to describe a laser beam weld.
- Larger spot diameter at equal power levels lead to larger grains in the weld, with loss in microhardness, UTS and elongation to fracture.
- Medium LBP and medium welding velocity lead to the best results. Excessive power input cannot be compensated by higher velocities, because higher power levels lead to worse results, as higher velocities do.

Acknowledgements

The authors thank Dr. Mok-Young Lee and Hung-Gyoo Lee of RIST, Research Institute of Industrial Science & Technology, for providing the sheet material and Mr. Falk Dorn from HZG, WMF for the metallography.

References

- [1] N. Kashaev, S. Riekehr, M. Horstmann and V. Ventzke: Fatigue, Fatigue Crack Propagation and Mechanical Fracture Behaviour of Laser Beam-Welded AZ31 Magnesium Sheets, *Materials Science Forum* 783-786 (2014) 2310-2315, doi:10.4028/www.scientific.net/MSF.783-786.2310
- [2] P. Srinivasan, S. Riekehr, C. Blawert, W. Dietzel and M. Kocak, 'Mechanical properties and stress corrosion cracking behaviour of AZ31 magnesium alloy laser weldments,' *Trans. Nonferrous Met. Soc. China*, no. 21 (2011) 1-8.
- [3] H. Haferkamp, F. von Alvensleben, I. Burmester, and M. Niemeyer: *Proc. ICALEO 97*, Laser Institute of America, Orlando, FL, 1997.
- [4] Z. Wang, M. Gao, H. Tang and X. Zeng: 'Characterization of AZ31B wrought magnesium alloy joints welded by high power fibre laser', *Materials Characterization*, no. 62 (2011) 943-951.
- [5] N. Hort, R. Schmidt-Fetzer: Project of the DFG: 'Elaboration of a model for the viscosity of liquid alloys with predictive capability by implementation of consistent thermodynamic descriptions and validation by experimental investigation of liquid magnesium alloys', Project duration till End of 2015